Hue University Journal of Science: Natural Science
Vol. 133, No. 1B, 99–108, 2024

pISSN 1859-1388
eISSN 2615-9678

Fabrication and evaluation of some electrochemical properties of screen-printed electrodes for use in electrochemical analysis

Hoang Thai Long[1]*, Phan Trung Ngoc[1,2], Ho Xuan Anh Vu[1], Nguyen Dang Giang Chau[1], Ho Van Minh Hai[1]

[1] Department of Chemistry, University of Sciences, Hue University, 77 Nguyen Hue St., Hue, Vietnam
[2] Center for Disease Control of Thua Thien Hue Province, 10-12 Nguyen Van Cu St., Hue, Vietnam

* Correspondence to Hoang Thai Long <hthailong@hueuni.edu.vn>

(*Received: 01 June 2023; Revised: 25 July 2023; Accepted: 03 August 2023*)

Abstract. Three types of conductive inks, including Ceres, Acheson carbon inks, and Ag/AgCl ink, were utilized to fabricate screen-printed electrodes (SPEs) on a 0.4 mm thick polyethylene terephthalate substrate using a screen-printing technique. To enhance the electrical conductivity, the printed electrodes were cured at 80 °C for 90 minutes. The basic electrochemical properties of the self-made SPEs using these conductive inks were determined, evaluated, and compared with commercial SPEs from Metrohm. Although the electroactive surface areas of the self-made SPEs were not significantly different from those of the commercial SPEs, the heterogeneous electron transfer rates on the surfaces of self-made SPEs using Ceres and Acheson inks were inferior to those of the commercial SPEs. However, after pre-condition by applying a potential of +1.2 V for 180 s in a 2 M Na_2CO_3 solution, the electrochemical properties of the self-made SPEs, including the active surface areas and heterogeneous electron transfer rates, were significantly improved and became better than those of the commercial SPEs.

Keywords: screen-printed electrode, SPE, cyclic voltammetry, electroactive surface area, electron transfer rate

1 Introduction

In addition to spectroscopic methods, heavy metals and many organic compounds can be quantified by various electroanalytical methods. One of the most notable advantages of electroanalytical methods is the ability to downsize devices for on-site analysis. Small analytical devices consume less energy and chemicals, thus contributing to environmental protection [1].

To meet the demand for downsized electro-analytical devices, in the late 1980s, a new type of electrode was developed based on the principle of using carbon-based conductive ink to print electrodes on polymer sheets, ceramics, or even paper using screen printing techniques. This electrode, known as a screen-printed electrode (SPE), has attracted the attention of many scientists since its inception. Many studies on material improvement, fabrication techniques, and analytical applications have been carried out over the past three decades with this type of electrode [2, 3]. Currently, graphite and carbon black are the most commonly used materials for the fabrication of SPEs. SPEs are compact but include the working electrode, reference electrode, and auxiliary electrode, which can replace the complex three-electrode system used in traditional electroanalytical methods. Due to their small size, only a very small sample volume is required for analysis, usually only a few drops

of solution, which increases mass transfer rate, reduces noise, and allows for fast analysis. In addition, due to their low cost, SPEs are often produced for one-time use, without requiring electrode treatment, cleaning, polishing, etc. [4].

This paper presents the results of a study on the conditions for fabricating screen-printed electrodes (SPEs) on plastic substrates using carbon based and Ag/AgCl conductive inks and evaluates the basic electrochemical properties of the SPEs that were fabricated.

2 Experimental

2.1 Materials and chemicals

The carbon black conductive ink Ceres YT-581 screen printing ink from Guangzhou Print Area Technology Co. (China) and the Acheson ED-423SS Graphite Based Polymer Thick Film Ink from Eisho Electronic Materials Co. (China) were used. Silver/silver chloride (60/40) paste for screen printing was purchased from Sigma-Aldrich (Germany). $K_3[Fe(CN)_6]$ and $K_4[Fe(CN)_6]$ were purchased from Sigma-Aldrich (Germany). HNO_3, HCl, Na_2CO_3, KCl were from Merck (Germany); all chemicals were of analytical grade. Chemical solutions were prepared with double-distilled water. PET (polyethylene terephthalate) sheets with a thickness of 0.2 mm, 0.3 mm, and 0.4 mm from HUNUFA (Vietnam) were used as substrates for electrode printing. The screen mesh was made of polyester fibers with a mesh size of T90, T100, and T120 from Hebei Reking Wire Mesh (China). A self-made screen printing table with a wooden base, glass plate, and metal frame clamps was used for electrode printing.

2.2 Instrumentation

Electrochemical measurements were carried out on the Metrohm DropSens μSTAT-400 handheld bipotentiostat/galvanostat (Switzerland) controlled by the DropView 4000 software. The Thermo-Scientific Heratherm OGH100 oven (Germany) was used for electrode curing experiments. The Sanwa CD800a digital multimeter (Taiwan) was used to measure the resistance of the SPEs. The Metrohm DropSens 11L electrode (Switzerland) was used as a reference electrode for comparison with the self-made electrodes.

2.3 Screen printing process for SPE fabrication

SPEs are fabricated by screen-printing two conductive ink layers of Ag/AgCl and carbon onto a PET plastic sheet. The design of the SPE pattern is created using CorelDraw software and printed onto a clear acetate film. A negative stencil is created on the photosensitive emulsion-coated mesh screen. The conductive ink is then used to print the SPE onto the PET sheet that has been cleaned with soap, water, and acetone. The reference electrode and electrical pathways are pre-printed with Ag/AgCl ink and allowed to air-dry.

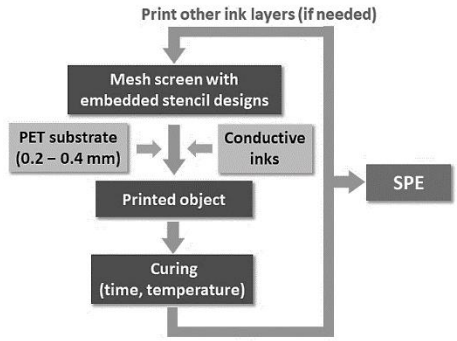

Fig. 1. Process for SPE fabrication

Then, use carbon based conductive ink to print the working electrode and counter electrode on top of the previously printed Ag/AgCl ink layer. After printing, the SPE is cured at an appropriate temperature and time. Finally, a layer of insulation coating is applied to the electrode to prevent electrical shorting at the electrode contact

pISSN 1859-1388
eISSN 2615-9678

region when immersed in the test solution. The process of fabricating an SPE electrode and the component ink layers of the SPE are illustrated in Fig. 1 and Fig. 2.

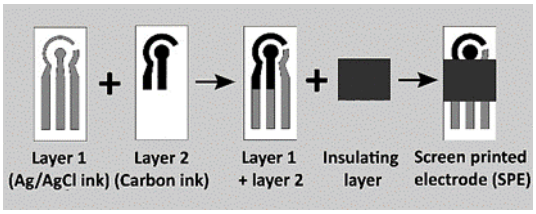

Fig. 2. Component layers of an SPE

2.4 Temperature effects

The influence of temperature on the deformation of PET substrate and the resistance of the ink layer was examined by thermal curing the samples in a drying oven with a temperature control accuracy of ±1 °C. The deformation of plastic sheets (size: 4.5 cm × 4.5 cm; thickness: 0.2 mm, 0.3 mm, and 0.4 mm) after curing was visually classified and each experiment was repeated twice.

The resistance of the ink layer after curing was measured using a two-point resistance measurement method [5] with a digital multimeter at four different random locations on the ink layer with a measuring distance of 1 cm, and the average resistance was calculated. The test samples were 0.4 mm thick PET sheets with rectangular ink strips (8 mm × 40 mm) printed using T100 mesh (100 threads per cm). The samples were left to dry naturally for about 15 minutes before curing.

2.5 Effect of mesh size on ink layer resistance

The effect of mesh size on the resistance of the ink layer was evaluated by measuring the resistance of ink layers printed using different mesh sizes, namely T90, T100, and T120 (where T90 corresponds to 90 threads per centimeter...), using the two-point resistance measurement method described in section 2.4. The resistance measurement was repeated four times at four different locations on the ink layer.

2.6 SPE pre-condition (electrochemical activation pre-treatment) mode

After heat treatment, SPEs are typically further pre-conditioned to enhance their electrochemical properties. In this study, only self-made Ceres ink-printed SPEs were tested by applying a positive potential in a Na_2CO_3 solution for a certain period of time [6]. After pre-condition, the cyclic voltammogram (CV) of the SPE in a mixture of 4 mM $K_3[Fe(CN)_6]$ + 4 mM $K_4[Fe(CN)_6]$ + 0.5 M KCl solution (referred to as Fe^{III}/Fe^{II}-KCl solution) was recorded. The anodic peak current (I_{pA}) and cathodic peak current (I_{pC}) on the CV curves were used as criteria for selecting the pre-condition modes, including the Na_2CO_3 concentration, potential, and pre-condition time.

2.7 Electroactive surface area of the electrode

The electroactive surface area of the electrode is determined based on the Randle-Sevcik equation, Eq.(1) [7, 8]:

$$I_p = (2.69 \times 105) \cdot n^{3/2} \cdot D^{1/2} \cdot v^{1/2} \cdot A \cdot C \quad (1)$$

where I_P: peak current (A); n: number of electrons transferred by the analyte; D: diffusion coefficient of the electroactive species (cm^2/s); v: scan rate (V/s); A: electroactive surface area of the electrode (cm^2); C: concentration of the electroactive species in solution (mol/cm^3). For a defined redox couple:

$$I_p = K \times v^{1/2} \quad (2)$$

where: $$K = (2.69 \times 10^5) \cdot n^{3/2} \cdot D^{1/2} \cdot A \cdot C \quad (3)$$

The CV of the SPE is recorded in a solution of Fe^{III}/Fe^{II}-KCl over a potential range of −0.15 V to 0.8 V at scan rates from 20 mV/s to 100 mV/s. From the values of I_{pC} measured on the CVs at different scan rates, a linear correlation equation between I_{pC} and $v^{1/2}$, Eq. (2), can be established. The slope of this linear equation is the value of K

in Eq. (3). For the redox couple in use, n is 1 and the D of $K_3[Fe(CN)_6]$ is 7.60×10^{-6} cm^2/s [8], so A of the electrode can be calculated from Eq. (3).

2.8 Heterogeneous electron transfer rate

The heterogeneous electron transfer rate on the electrode surface (referred to as electron transfer rate) is evaluated through peak current, peak potential, and CV shape of self-made electrodes using two types of conductive inks (Ceres and Acheson) and the DropSens printed electrode from Metrohm in Fe^{III}/Fe^{II}-KCl solution at one or several different scan rates.

3 Results and Discussion

3.1 Curing conditions

This study used PET plastic as the substrate for fabricating SPEs because the ink can adhere well to this material's surface [9]. Moreover, PET plastic has good chemical resistance and is not affected by strong acidic or alkaline environments. This can help increase the number of times the SPE can be reused. After printing the conductive ink on PET plastic, the product needs to be treated with heat. During this process, the solvent will evaporate, the binding material in the ink will be polymerized and crosslink or decompose [10], reducing the distance between the conductive material particles and thus improving the electrochemical properties of the electrode surface [11]. However, since the substrate layer used to manufacture the SPE is PET plastic, it may deform at high temperatures, thereby changing the shape of the electrode and potentially causing cracking, peeling of the conductive ink layer. Therefore, it is necessary to investigate and select appropriate curing conditions.

Effect of curing temperature on the deformation of PET plastic sheet

The experimental results showed that PET sheets with thicknesses of 0.2 mm and 0.3 mm were deformed after 10 minutes of curing at temperatures of 60 °C and 65 °C, respectively. The 0.4 mm PET sheet did not deform when cured at 85 °C for less than 30 minutes. After 6 hours of curing at 80 °C, the 0.4 mm PET sheet still did not deform. Therefore, the 0.4 mm PET plastic sheet and a maximum curing temperature of 80 °C were chosen for further experiments.

Effect of curing temperature on the resistance of ink layer

The resistance of Ceres and Acheson ink layers decreased gradually with increasing curing time at 80 °C from 0 min to 150 min.

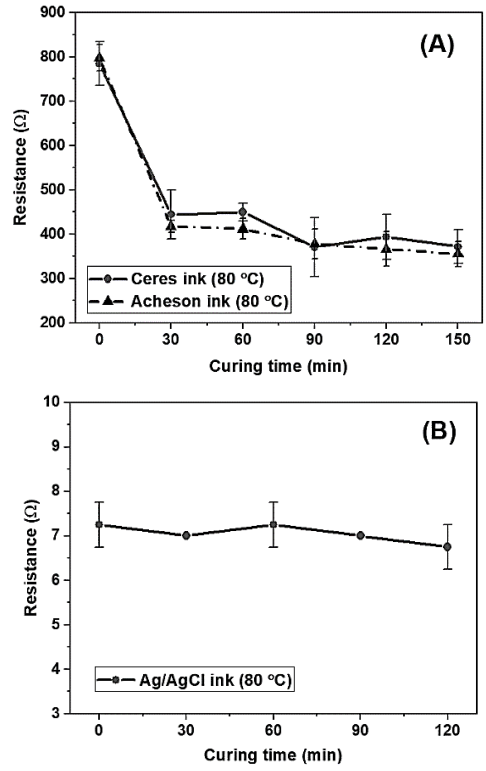

Fig. 3. Effect of temperature and curing time on the resistance of Ceres and Acheson ink layers (A) and Ag/AgCl ink layer (B) (bars represent ±*SD*, n = 4)

pISSN 1859-1388
eISSN 2615-9678

The resistance decreased rapidly after 30 minutes and did not change significantly after 90 minutes (Fig. 3A). Therefore, to obtain good electrical conductivity of the SPE product when using these types of inks, the SPE should be cured for at least 90 minutes at 80 °C after printing.

The resistance of Ag/AgCl ink layer was low and almost unchanged during the curing process (Fig. 3B). Therefore, after printing with Ag/AgCl ink, it is only necessary to let it dry naturally without heat treatment.

Effect of screen mesh fineness on the resistance of the ink layer

As the screen mesh fineness increased, the resistance of the ink layer decreased (Table 1). The high fineness of the screen mesh allows for a sharper image, but it reduces the amount of ink passing through the mesh to adhere to the substrate, thus decreasing the thickness of the ink layer and increasing its resistance (reducing its conductivity) [12]. To obtain SPEs with both sharp images and low resistance, the T100 mesh was chosen for use.

Table 1. Effect of screen mesh fineness on the resistance of the ink layer

Runs	Resistance (Ω)					
	T90 mesh		T100 mesh		T120 mesh	
	Ceres	Acheson	Ceres	Acheson	Ceres	Acheson
1	321	331	350	358	394	401
2	317	308	346	372	403	412
3	342	325	370	378	389	394
Mean ± *SD*	326.7 ± 13.4	321.3 ± 11.9	355.3 ± 12.9	369.3 ± 10.3	395.3 ± 7.1	402.3 ± 9.1

(Curing conditions: 80 °C, 90 min)

3.2 SPE pre-condition mode

After printing, the thermal curing process has evaporated the solvent, dried the adhesive material, brought the conductive particles closer together, and increased the conductivity of the ink layer on the SPE [10, 11]. However, at this stage, there still remains a significant amount of solidified adhesive material dispersed among the conductive particles, affecting the rate of electron transfer at the working electrode surface [6].

Pre-conditioning the SPE through chemical or electrochemical methods in an acidic or alkaline medium can remove the non-conductive components on the electrode surface and improve the electrochemical properties of the SPE [6].

To find suitable pre-condition mode, the SPEs were immersed in H_2SO_4, NaOH, Na_2CO_3 solutions, and subjected to a positive potential. Preliminary experimental results showed that soaking the SPE fabricated with Ceres ink (SPE-C) in NaOH solution and electrochemically pre-conditioning it in Na_2CO_3 solution significantly improved their electrochemical properties.

Although the process is simple, after chemical pre-condition by soaking in 2 M NaOH solution for approximately two hours, the conductive ink layer on the SPE-C showed signs of peeling, which did not occur with the electrochemical pre-condition in 2 M Na_2CO_3 solution. Further experimental investigations revealed that electrochemical pre-condition by applying a potential of +1.2 V to SPE-C in 2 M Na_2CO_3 solution for 180 s significantly increased

the peak currents (I_{pA} and I_{pC}) of the CV curve of the Fe^{III}/Fe^{II}-KCl solution recorded on the pre-conditioned SPE-C (SPE-C-PT) (Fig. 4). Therefore, these pre-condition parameters were selected for subsequent experiments.

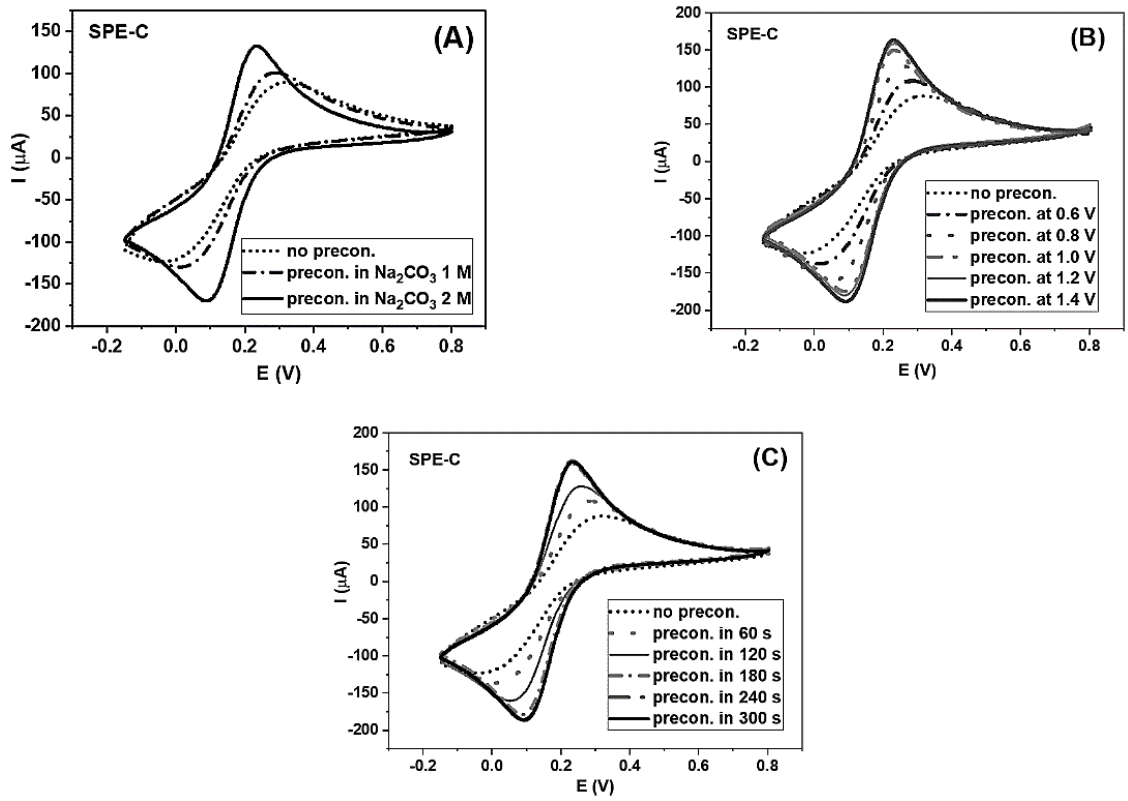

Fig. 4. The CV curves of the Fe^{III}/Fe^{II}-KCl solution recorded on the pre-conditioned SPE-Cs: (A) in 1 M and 2 M Na_2CO_3 at +1.2 V, 120 s; (B) in 2 M Na_2CO_3, 120 s, at potentials ranging from 0.6 V to 1.4 V; (C) in 2 M Na_2CO_3 at +1.2 V, with time intervals ranging from 60 s to 300 s

3.3 Electroactive surface area of the electrode

The electroactive surface area of the electrode is an important parameter that affects the electrochemical properties of the electrode. According to the Randle-Sevcik equation (1), it can be observed that the peak current (I_P) of the analyte increases linearly with the electroactive surface area (A). Therefore, a larger A value corresponds to a higher I_P, indicating better sensitivity for the analysis. The determined electroactive surface areas of SPE-C, Acheson ink printed electrode (SPE-A), DropSens 11L electrode from Metrohm (SPE-D), and pre-conditioned SPE-C (SPE-C-PT) are presented in Table 2 along with their geometric surface areas.

The electroactive surface areas (A) of SPE-C and SPE-A are approximately equal and not significantly smaller than that of SPE-D (about 1.1 times).

It is worth noting that the electroactive surface area of all three types of electrodes, SPE-C, SPE-A, and SPE-D, is smaller than their geometric surface area (about 1.3 times). This may be due to non-conductive or poorly conductive adhesive materials remaining in the ink layer of the electrode, which reduces the recorded electrochemical signals and thus decreases A. This can be addressed by electrode treatment as

pISSN 1859-1388
eISSN 2615-9678

described in section 3.2. The electroactive surface area of the pre-conditioned SPE-C electrode (SPE-C-PT) has increased by approximately three times compared to the *A* of SPE-C, SPE-A, and SPE-D, and is nearly 2.5 times the geometric surface area of these electrodes.

Table 2. The electroactive surface area and geometric surface area of the investigated SPEs.

Electrodes	Electroactive surface area (cm^2) (Mean ± *SD*, n = 3)	Geometric surface area (cm^2)
SPE-C	0.0993 ± 0.0010	**0.1257**
SPE-A	0.0997 ± 0.0012	
SPE-D	0.1086 ± 0.0014	
SPE-C-PT	0.3111 ± 0.0010	

3.4 Electron transfer rate on the electrode surface

The fabrication process and techniques of SPE can strongly influence its electrochemical properties. In addition to the electroactive surface area, the electron transfer rate on the electrode surface is an important electrochemical characteristic directly affecting the analytical signal of the electrode. Various methods can be used to evaluate these properties of SPE [13, 14, 15]. In this study, the CV curves of Fe^{III}/Fe^{II}-KCl solution were recorded on different types of SPEs to assess the electron transfer rate on the electrode surface. A slower electron transfer rate on the electrode surface is reflected by broader anodic and cathodic peaks on the CV curve, lower anodic peak current (I_{pA}) and cathodic peak current (I_{pC}), a larger ratio of I_{pA}/I_{pC} deviating from the value of 1, and a larger peak separation (ΔE_p) between the anodic and cathodic peaks (indicating a less reversible oxidation and reduction process of the redox couple) [8, 14, 15]. The anodic and cathodic peaks on the CV curve also undergo more shifting when the scan rate is varied [16], resulting in less sensitive analytical signals on these electrodes.

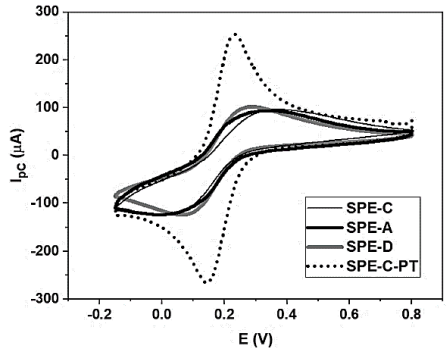

Fig. 5. The CV curves of the Fe^{III}/Fe^{II}-KCl solution on SPE-C, SPE-A, SPE-D, and SPE-C-PT (potential range: −0.15 V to +0.8 V, scan rate: 100 mV/s)

From the CV curves (Fig. 5) of Fe^{III}/Fe^{II}-KCl solution recorded at a scan rate of 100 mV/s on SPE-C, SPE-A, SPE-D, and SPE-C-PT, several key parameters can be determined to evaluate the electrodes (Table 3).

Table 3. Some key parameters determined from the CV curves used to evaluate the electrodes.

Electrodes	SPE-C	SPE-A	SPE-D	SPE-C-PT
E_A **(mV)**	0.370	0.342	0.286	0.230
E_C **(mV)**	−0.004	−0.004	0.066	0.144
ΔE_p **(mV)**	**0.374**	**0.328**	**0.220**	**0.086**

Electrodes	SPE-C	SPE-A	SPE-D	SPE-C-PT
I_{pA} (μA)	52.280	40.702	97.863	247.631
I_{pC} (μA)	117.801	113.991	134.264	274.049
I_{pA}/I_{pC}	**0.444**	**0.357**	**0.729**	**1.002**

(Potential range: −0.15 V to 0.8 V; Scan rate: 100 mV/s)

The ΔE_P values of SPE-C and SPE-A electrodes are not significantly different and are both larger than the ΔE_P value of SPE-D. The ratio of I_{pA}/I_{pC} for SPE-D is also closer to a value of 1 compared to the ratio of SPE-C and SPE-A. This indicates that the electron transfer rate of the redox process on the surface of SPE-C and SPE-A electrodes is lower than that on SPE-D.

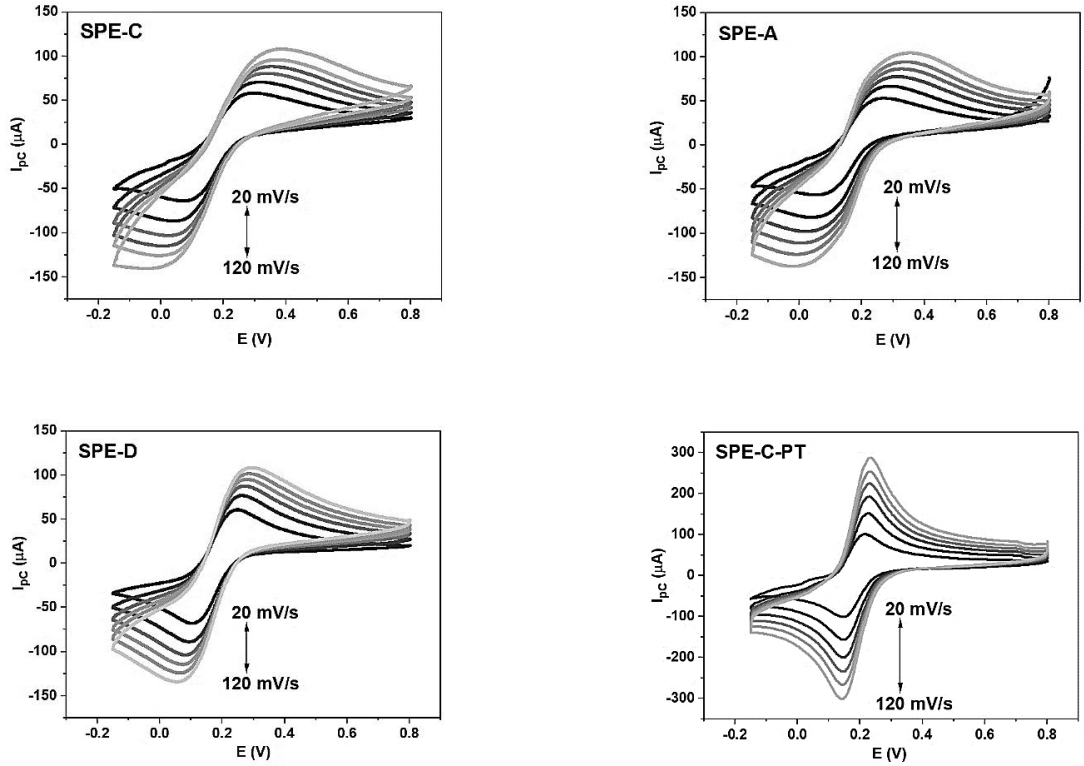

Fig. 6. CV curves of Fe^{III}/Fe^{II}-KCl solution recorded on SPE-C, SPE-A, SPE-D, and SPE-C-PT electrodes at scan rates ranging from 20 mV/s to 120 mV/s

However, after the pre-condition of SPE-C (+1.2 V, 2 M Na_2CO_3, 180 s), the anodic and cathodic peaks on the CV curve of SPE-C-PT showed significant changes compared to the untreated electrodes. The ΔE_P ratio of SPE-C-PT is 0.086, much smaller than the corresponding values of SPE-C, SPE-A, and SPE-D, and very close to the theoretical ΔE_P value for the investigated redox couple of 0.059 V. The ratio of I_{pA}/I_{pC} determined on SPE-C-PT is nearly equal to 1. The anodic and cathodic peaks on the CV curve show significant shifts when changing the scan rate for SPE-C, SPE-A, and SPE-D electrodes, but they hardly shift for the SPE-C-PT electrode (Fig. 6). The anodic and cathodic peaks on the CV curves recorded on SPE-C-PT are sharp and not broadened as seen on the CV curves using electrodes without pre-conditioning.

pISSN 1859-1388
eISSN 2615-9678

Therefore, compared to the Metrohm (SPE-D) electrode, the self-made (SPE-C and SPE-A) electrodes have a relatively similar electroactive surface area but exhibit lower electron transfer rates on their surfaces. However, after the pre-condition, the basic electrochemical characteristics of the self-made electrode have been significantly improved.

4 Conclusions

This article presents the suitable conditions for fabricating screen-printed electrodes using carbon conductive ink and Ag/AgCl conductive ink on a PET plastic substrate. After pre-condition at +1.2 V for 180 seconds in a 2 M Na_2CO_3 solution, the self-fabricated screen-printed electrode exhibited good fundamental electrochemical properties and can be used for electrochemical analysis.

Acknowledgments

This research is funded by Hue University under Decision 176/QĐ-ĐHH, Code number DHH2021-01-187.

References

1. Renedo OD, Alonso-Lomillo MA, Martínez MJA. Recent developments in the field of screen-printed electrodes and their related applications. Talanta. 2007;73(2):202-19.
2. Hart JP, Wring SA. Screen-printed voltammetric and amperometric electrochemical sensors for decentralized testing. Electroanalysis. 1994;6(8):617-24.
3. Liu X, Yao Y, Ying Y, Ping J. Recent advances in nanomaterial-enabled screen-printed electrochemical sensors for heavy metal detection. TrAC Trends in Analytical Chemistry. 2019;115:187-202.
4. González-Costas JM, Gómez-Fernández S, García J, González-Romero E. Screen-printed electrodes-based technology: Environmental application to real time monitoring of phenolic degradation by phytoremediation with horseradish roots. Science of The Total Environment. 2020;744:140782.
5. Phillips C, Al-Ahmadi A, Potts S-J, Claypole T, Deganello D. The effect of graphite and carbon black ratios on conductive ink performance. Journal of Materials Science. 2017;52(16):9520-30.
6. Cui G, Yoo JH, Lee JS, Yoo J, Uhm JH, Cha GS, et al. Effect of pre-treatment on the surface and electrochemical properties of screen-printed carbon paste electrodes. Analyst. 2001;126(8):1399-403.
7. García-Miranda Ferrari A, Foster CW, Kelly PJ, Brownson DAC, Banks CE. Determination of the Electrochemical Area of Screen-Printed Electrochemical Sensing Platforms. Biosensors. 2018;8(2).
8. Zhu P, Zhao Y. Cyclic voltammetry measurements of electroactive surface area of porous nickel: Peak current and peak charge methods and diffusion layer effect. Materials Chemistry and Physics. 2019;233:60-7.
9. Willfahrt A, Fischer T, Huebner G. Improving the electrical performance and mechanical properties of conductive ink on thin compound substrate. Journal of Print and Media Technology Research. 2016;5:7-14.
10. Fletcher S. Screen-Printed Carbon Electrodes. Electrochemistry of Carbon Electrodes. Electrochemistry of Carbon Electrodes. Wiley; 2015. p. 425-44.
11. Suresh RR, Lakshmanakumar M, Arockia Jayalatha JBB, Rajan KS, Sethuraman S, Krishnan UM, et al. Fabrication of screen-printed electrodes: opportunities and challenges. Journal of Materials Science. 2021;56(15):8951-9006.
12. Joyce M, Pal L, Hicks R, Agate S, Williams TS, Ray G, et al. Custom tailoring of conductive ink/substrate properties for increased thin film deposition of poly(dimethylsiloxane) films. Journal of Materials Science: Materials in Electronics. 2018;29(12):10461-70.
13. Foster CW, Kadara RO, Banks CE. Fundamentals of Screen-Printing Electrochemical Architectures. In: Banks CE, Foster CW, Kadara RO, editors. Screen-Printing Electrochemical Architectures. Cham: Springer International Publishing; 2016. p. 13-23.
14. Harris AR, Newbold C, Cowan R, Wallace GG. Insights into the Electron Transfer Kinetics, Capacitance and Resistance Effects of Implantable Electrodes Using Fourier Transform AC Voltammetry on Platinum. Journal of The Electrochemical Society. 2019;166(12):G131

15. Wang J, Tian B, Nascimento VB, Angnes L. Performance of screen-printed carbon electrodes fabricated from different carbon inks. Electrochimica Acta. 1998;43:3459-65.

16. Wang J. Analytical Electrochemistry. 3rd ed. USA: John Wiley & Sons; 2006.